Research Article

Optimum Design of a Nonlinear Vibration Absorber Coupled to a Resonant Oscillator: A Case Study

H. F. Abundis-Fong [iD],[1] J. Enríquez-Zárate,[2] A. Cabrera-Amado,[3] and G. Silva-Navarro[4]

[1]*Unidad Especializada en Energías Renovables, Instituto Tecnológico de la Laguna, Tecnológico Nacional de México, 27400 Torreón, COAH, Mexico*
[2]*Facultad de Ingeniería, Universidad Panamericana, Josemaría Escrivá de Balaguer 101, 20290 Aguascalientes, AGS, Mexico*
[3]*Universidad del Papaloapan, 68400 Loma Bonita, OAX, Mexico*
[4]*Centro de Investigación y de Estudios Avanzados del IPN, Departamento de Ingeniería Eléctrica, Sección de Mecatrónica, 07360 Ciudad de México, Mexico*

Correspondence should be addressed to H. F. Abundis-Fong; habundis@correo.itlalaguna.edu.mx

This paper presents the optimal design of a passive autoparametric cantilever beam vibration absorber for a linear mass-spring-damper system subject to harmonic external force. The design of the autoparametric vibration absorber is obtained by using an approximation of the nonlinear frequency response function, computed via the multiple scales method. Based on the solution given by the perturbation method mentioned above, a static optimization problem is formulated in order to determine the optimum parameters (mass and length) of the nonlinear absorber which minimizes the steady state amplitude of the primary mass under resonant conditions; then, a PZT actuator is cemented to the base of the beam, so the nonlinear absorber is made active, thus enabling the possibility of controlling the effective stiffness associated with the passive absorber and, as a consequence, the implementation of an active vibration control scheme able to preserve, as possible, the autoparametric interaction as well as to compensate varying excitation frequencies and parametric uncertainty. Finally, some simulations and experimental results are included to validate and illustrate the dynamic performance of the overall system.

1. Introduction

Vibration is a constant problem as it can impair performance and lead to fatigue, damage, and failure of a structure. Control of vibration is a key factor in preventing such detrimental results. There are cases when vibrations are desirable, such as in certain types of machine tools or production lines. Most of the time, however, the vibration of mechanical systems is undesirable as it wastes energy, reduces efficiency, and may be harmful or even dangerous [1]. Engineers and scientists are constantly working to develop more complex theoretical foundations for understanding vibration problems and to have better tools to analyze, measure, and eliminate the vibrations of mechanical systems. Vibration attenuation techniques are often utilized to increase the energy dissipation of

systems and structures. In this way the response of a structure driven at resonant frequencies may be greatly decreased.

A popular way to deal with vibration attenuation is carried out by (linear or nonlinear) passive techniques, taking advantage of the physical properties of the system itself, where the engineering approach to avoid the undesirable effects of mechanical vibrations is to modify mass, stiffness, and damping properties of structures with respect to the primary configuration of the system. Within the passive vibration control approach there is the linear Tuned Mass Damper (TMD), which is an efficient passive vibration suppression device comprising a mass, springs, and viscous damper. TMD has been widely used in machinery, buildings, and civil structures. Extensive research on TMD has been carried out, where definitively one of the priorities has been

to determine optimum tuning between absorber and primary system with the aim of obtaining the highest percentage of possible vibration absorption [2–5].

On the other hand, the study of passive vibration control using nonlinear devices is an interesting subject, because of the phenomena that may occur and do not happen in their linear counterparts [6–9]. There is a special class of nonlinear vibration absorbers called autoparametric absorbers which are characterized by nonlinear internal coupling that involves at least two vibration modes. This condition results in energy transfer from one mode to another one [10]. From the pioneering work done by Haxton and Barr [11], these types of systems have been studied by several researches due to the dynamic characteristics present when they are tuned to a primary system. From the point of view of passive control, autoparametric absorbers have been designed to mitigate resonant vibrations. Cartmell and Roberts [12] illustrated the highly complex responses that can be generated on two coupled cantilever beams when two internal resonances exist in very close proximity to each other. Cartmell and Lawson [13] showed that it is possible to improve the response performance of an autoparametric vibration absorber by introducing a limited form of intelligent control. The dynamic response of a beam-tip mass-pendulum system subjected to a sinusoidal excitation was investigated by Cuvalci and Ertas [14], where the nonlinear equations of motion were developed to investigate the autoparametric interaction between the first two modes of the overall system. Furthermore, Vyas and Bajaj [15] analyzed the dynamics of a resonantly excited single-degree-of-freedom linear system coupled to an array of nonlinear autoparametric vibration absorbers; they demonstrated analytically that it is possible to improve the absorber bandwidth using a multiple array of pendulums. Recently, significant research has been carried out into the area of autoparametric system. Vazquez-Gonzalez and Silva-Navarro discussed the dynamic response and nonlinear frequency analysis of a damped Duffing system attached to an autoparametric pendulum absorber, operating under the external and internal resonance conditions [16]. Silva-Navarro et al. described experimental studies of an active autoparametric absorber using a PZT patch actuator to attenuate resonant vibrations in a Duffing oscillator and a building-like structure [17, 18]. Yan et al. [19] investigated the nonlinear characteristics of an autoparametric vibration system. They established that depending on the application of such a system, its complex dynamic behavior could be exploited or avoided.

In this paper, we propose a way to select the optimal parameters of a passive autoparametric cantilever beam absorber based on the nonlinear frequency response of the complete system which is obtained using the method of multiple scales. Then, we consider the synthesis of an active nonlinear absorber, with a small PZT patch actuator, to be used on primary system. The active vibration absorber employs feedback information from the primary system and the beam absorber, feedforward information from the excitation force and on-line computations from the nonlinear
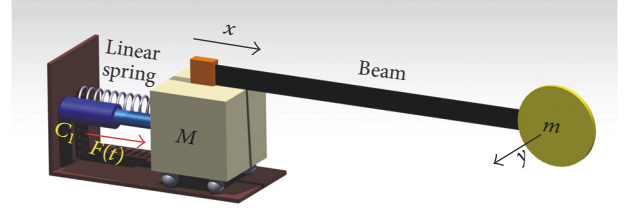

FIGURE 1: Schematic diagram of the primary system with autoparametric absorber.

approximate frequency response, parameterized in terms of the equivalent stiffness of the PZT actuator, thus providing a mechanism to asymptotically tune an optimal and stable attenuation solution.

2. System Description

Figure 1 shows a schematic diagram of the mechanical system. The primary system consists of a linear spring mass system with viscous damping and it is excited by an external harmonic force $F(t) = F_0 \cos \Omega t$, with amplitude F_0 and excitation frequency Ω. In order to mitigate the harmonic vibrations generated by $F(t)$, an autoparametric cantilever beam vibration absorber (secondary system) is used.

The nonlinear absorber is composed by a thin beam attached over the primary system and with an equivalent mass m at the end with lateral motion restricted to a horizontal plane (i.e., gravity effects are not considered). The length l denotes the beam total length and c_2 is a small viscous damping on the beam. Both primary and secondary subsystems are coupled by means of the inertia that resulted from the beam attachment; besides, because the entire system lacks any kind of actuators, it results in a purely passive vibration control scheme.

2.1. Equations of Motion. The equations of motion for the two-degree-of-freedom system consisting of the linear oscillator and the passive autoparametric cantilever beam absorber are obtained via Euler–Lagrange formulation. The total kinetic and potential energies are described as

$$T = \frac{1}{2}M\dot{x}^2 + \frac{1}{2}m\dot{y}^2 + \frac{1}{2}m(\dot{w} - \dot{x})^2,$$

$$V = \frac{1}{2}kx^2 + \left(\frac{3EI}{2l^3}\right)y^2,$$

(1)

where $w = 3y^2/5l$ denotes the axial (contraction) displacement of the tip mass m, along the x direction, which is directly related to the lateral displacement y of the same tip mass. Note that the potential energy is only bending strain energy. The equations of motion of the overall system are obtained by computing the Lagrangian $L = T - V$ and developing the Euler–Lagrange equations, considering an external

harmonic force $F(t)$ and linear viscous dampings, as follows [11]:

$$(M + m)\ddot{x} + c_1\dot{x} + kx - \frac{6m}{5l}\left(y\ddot{y} + \dot{y}^2\right) = F(t),$$

$$m\ddot{y} + c_2\dot{y} + \left(\frac{3EI}{l^3} - \frac{6m}{5l}\ddot{x}\right)y + \frac{36m}{25l^2}y\left(y\ddot{y} + \dot{y}^2\right) = 0, \tag{2}$$

where x and y denote the longitudinal motion of the primary system and lateral displacement of the passive cantilever beam absorber, respectively. Furthermore, the parameters associated with the passive beam absorber are the modulus of Young E (aluminum), the area moment of inertia I, and the total length l. It is important to note the highly nonlinear and coupled system dynamics in (2). In essence, the beam absorber is inertially coupled to the primary system in such a way that proper tuning can lead to the autoparametric condition (two-mode nonlinear operation), where resonant harmonic forces can be attenuated.

In summary, the nonlinear vibration absorber is mounted on the main mass of the linear oscillator, oriented along x direction in such a way that its support is actually moving in the same direction. The transversal section of the beam is also arranged to yield a bending motion in the y (orthogonal to x direction). The nonlinear coupling between the forced primary system motion and the lateral (bending) motion on the beam is possible because there occurs the so-called parametric vibration phenomena on the cantilever beam, resulting in a kinetic energy transfer and, as a consequence, the lateral (bending) motion on the nonlinear vibration absorber.

3. System with Autoparametric Absorber

In order to get an approximate analytical solution for the nonlinear frequency response of the overall system, the equations of motion for the two-degree-of-freedom system (2) should be normalized by defining representative parameters. This task results in the following two coupled and nonlinear differential equations for the autoparametric beam absorber:

$$\ddot{x} + 2\varepsilon\zeta_1\omega_1\dot{x} + \omega_1^2 x - \varepsilon h\left(y\ddot{y} + \dot{y}^2\right) = \varepsilon f\cos(\Omega t),$$

$$\ddot{y} + 2\varepsilon\zeta_2\omega_2\dot{y} + \left(\omega_2^2 - \varepsilon g\ddot{x}\right)y + \varepsilon^2\beta y\left(y\ddot{y} + \dot{y}^2\right) = 0, \tag{3}$$

where the normalized system parameters are defined by

$$\omega_1^2 = \frac{k_1}{M + m},$$

$$2\varepsilon\zeta_1\omega_1 = \frac{c_1}{M + m},$$

$$\varepsilon h = \frac{6}{5l}\left(\frac{m}{M + m}\right),$$

$$\varepsilon f = \frac{F_0}{M + m},$$

$$\omega_2^2 = \frac{3EI}{ml^3},$$

$$2\varepsilon\zeta_2\omega_2 = \frac{c_2}{m},$$

$$\varepsilon g = \frac{6}{5l},$$

$$\varepsilon^2\beta = \frac{36}{25l^2},$$

$$\varepsilon = \frac{6\delta_0}{5l},$$

$$\delta_0 = \frac{F_0}{k_1}. \tag{4}$$

The small perturbation parameter ε considers the internal couplings between the cantilever beam absorber and the primary system, viscous dampings, nonlinearities, and external force into the system.

For the presence of autoparametric interaction between the primary system and the nonlinear absorber, by which the vibration absorption is obtained, the following expressions must be satisfied:

$$\Omega = \omega_1, \tag{5}$$

$$\omega_1 = 2\omega_2, \tag{6}$$

where Ω is the excitation frequency, ω_1 corresponds to the principal parametric frequency of the primary system, and ω_2 is the natural frequency of the cantilever beam absorber. These two expressions are well known as the external and internal resonance conditions, respectively.

3.1. Approximate Frequency Analysis. The method of multiple scales is used to compute an approximate solution (frequency response function) for the perturbed system (3) [20–22]. The perturbed solutions are expressed by $x = x_0(T_0, T_1) + \varepsilon x_1(T_0, T_1) + \cdots$ and $y = y_0(T_0, T_1) + \varepsilon y_1(T_0, T_1) + \cdots$, where $T_0 = t$ is the fast time scale, $T_1 = \varepsilon t$ is the slow time scale, and the remaining time scales are related by the perturbation as $T_n = \varepsilon^n t$, with $n = 0, 1, 2, \ldots$. Time derivatives along different time scales lead to differential operators $d/dt = D_0 + \varepsilon D_1 + \cdots$ and $d^2/dt^2 = D_0^2 + 2\varepsilon D_0 D_1 + \cdots$.

The external and internal resonance conditions, characterizing the autoparametric interaction between the two degrees of freedom, are perturbed as

$$\Omega = \omega_1 + \varepsilon\rho_1,$$

$$\omega_1 = \omega_2 + 2\varepsilon\rho_2, \tag{7}$$

where $\varepsilon\rho_1$ and $\varepsilon\rho_2$ define the external and internal detuning parameters, respectively.

Substituting the proposed first order solutions $x(T_0, T_1)$ and $y(T_0, T_1)$ into (3) and grouping the zero and first order terms in ε yield the set of partial differential equations:

$$\varepsilon^0 : D_0^2 x_0 + \omega_1^2 x_0 = 0, \tag{8}$$

$$\varepsilon^1 : D_0^2 x_1 + \omega_1^2 x_1 = -2\zeta_1 \omega_1 D_0 x_0 - 2D_0 D_1 x_0$$
$$+ hy_0 \left(D_0^2 y_0 \right) + h \left(D_0 y_0 \right)^2 \tag{9}$$
$$+ f \cos \left(\Omega T_0 \right),$$

$$\varepsilon^0 : D_0^2 y_0 + \omega_2^2 = 0, \tag{10}$$

$$\varepsilon^1 : D_0^2 y_1 + \omega_2^2 y_1 = g \left(D_0^2 x_0 \right) y_0 - 2D_0 D_1 y_0$$
$$- 2\zeta_2 \omega_2 D_0 y_0. \tag{11}$$

The proposed solutions in their polar forms are expressed as

$$x_0 = A \left(T_1 \right) e^{i\omega_1 T_0} + \overline{A} \left(T_1 \right) e^{-i\omega_1 T_0},$$
$$y_0 = B \left(T_1 \right) e^{i\omega_2 T_0} + \overline{B} \left(T_1 \right) e^{-i\omega_2 T_0}, \tag{12}$$

where the amplitudes depend on the slow time scale T_1 and the oscillations on the fast time scale T_0. Here $\overline{A}(T_1)$ and $\overline{B}(T_1)$ denote complex conjugates of the amplitudes $A(T_1)$ and $B(T_1)$, respectively. Substituting the proposed solutions in equations (9) and (11), removing secular terms, and using the polar forms

$$A \left(T_1 \right) = \frac{1}{2} a \left(T_1 \right) e^{i\delta(T_1)},$$
$$B \left(T_1 \right) = \frac{1}{2} b \left(T_1 \right) e^{i\gamma(T_1)} \tag{13}$$

leads to

$$- i\zeta_1 \omega_1^2 a - i\omega_1 a' + \omega_1 a \delta' - \frac{3}{8} \alpha a^3 - \frac{1}{2} h\omega_2^2 b^2 e^{i\phi_2}$$
$$+ \frac{1}{2} f e^{i\phi_1} = 0, \tag{14}$$

$$- \frac{1}{4} g\omega_1^2 abe^{-i\phi_2} - i\omega_2 b' + \omega_2 b\gamma' - i\zeta_2 \omega_2^2 b = 0,$$

where $\phi_1 = \rho_1 T_1 - \delta$ and $\phi_2 = 2\gamma - \delta - 2\rho_2 T_1$. Here a', b', δ', and γ' denote differentiation with respect to the slow time scale T_1.

The steady state responses of the overall system are computed for $a' = 0$, $b' = 0$, $\delta' = \rho_1$, and $\gamma' = \rho_1/2 + \rho_2$. The steady state responses are obtained by taking real and imaginary parts in (14) for the steady state conditions. Hence, by solving these equations the approximate amplitude responses for the primary and secondary subsystems are given by

$$a = \frac{4\omega_2^2}{(\varepsilon g) \omega_1^2} \sqrt{\left(\frac{\varepsilon \rho_1 + \omega_1}{2\omega_2} - 1 \right)^2 + \left(\varepsilon \zeta_2 \right)^2}, \tag{15}$$

$$0 = b^4 + Qb^2 + R, \tag{16}$$

TABLE 1: Simulation system parameters.

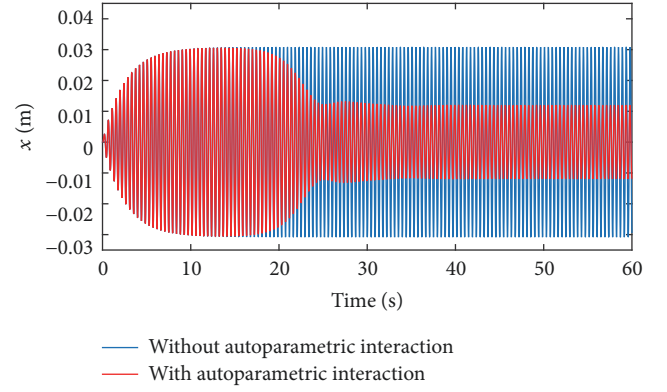| $M = 3.3502\,\text{kg}$	$k = 723\,\text{N/m}$	$c_1 = 2.8481\,\text{N/(m/s)}$
$c_2 = 0.072\,\text{N/(m/s)}$	$m = 0.23\,\text{kg}$	$l = 0.5324\,\text{m}$
$F_0 = 1.25\,\text{N}$	$\Omega = \omega_1 = 2.2\,\text{Hz}$	$\omega_2 = 1.1\,\text{Hz}$

FIGURE 2: Simulation response for the primary system with and without autoparametric interaction.

where

$$Q = \frac{16 \left(\varepsilon \zeta_1 \right) \left(\varepsilon \zeta_2 \right)}{(\varepsilon h) (\varepsilon g)} - \frac{8 \left(\Omega - 2\omega_2 \right) \left(\Omega - \omega_1 \right)}{(\varepsilon h) (\varepsilon g) \omega_1 \omega_2},$$

$$R = \frac{64 \left[\left(\Omega - \omega_1 \right)^2 + \omega_1^2 \left(\varepsilon \zeta_1 \right)^2 \right]}{(\varepsilon h)^2 (\varepsilon g)^2 \omega_1^2} \left[\left(\frac{\Omega}{2\omega_2} - 1 \right)^2 \right. \tag{17}$$

$$\left. + \left(\varepsilon \zeta_2 \right)^2 \right] - \frac{(\varepsilon f)^2}{(\varepsilon h)^2 \omega_2^4}.$$

3.2. Simulation Results.

Some simulations were performed in order to show the autoparametric phenomenon and therefore the passive vibration control in the primary system through the implementation of the proposed nonlinear absorber. The considered parameters of the complete system are given in Table 1. Note that the autoparametric vibration absorber is properly tuned with the external force because (5) and (6) are satisfied.

Figure 2 illustrates a comparison in the dynamic response of the primary system as a function of the autoparametric interaction. It is important to note that the percentage of vibration absorption is around 60% which can be increased as shown in the next section. On the other hand, the nonlinear absorber time history response, when there is autoparametric interaction, is described in Figure 3.

The frequency responses for both the primary and secondary systems, under autoparametric interaction and external harmonic force with amplitude $F_0 = 1.25$ N, are described in Figures 4 and 5, respectively. These responses are obtained directly from (15) and (16), with exactly tuning condition (i.e., $\varepsilon \rho = 0$). Here one can observe the consistency between the
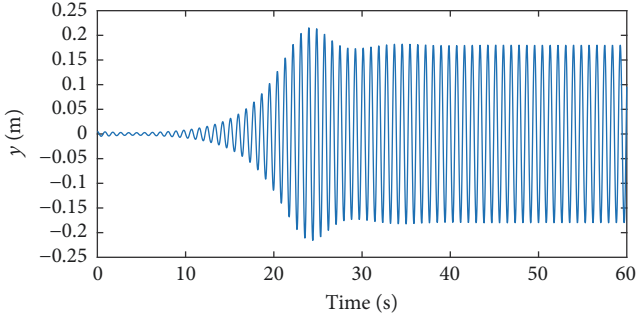
FIGURE 3: Simulation response for the secondary system when there is autoparametric interaction.
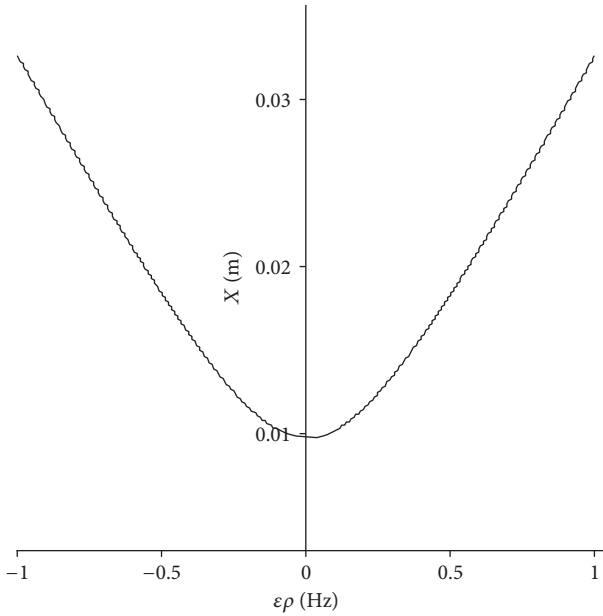

FIGURE 5: Frequency response for the autoparametric absorber.

FIGURE 4: Frequency response of the primary system.

frequency responses and the steady state dynamic behavior predicted in Figures 2 and 3.

4. Optimum Nonlinear Vibration Absorber

Even when the autoparametric vibration absorber treated in the previous section works to attenuate the mechanical vibrations in the primary system, it is convenient to carry out a study to determine its main parameters (length and mass) by which the maximum percentage of vibration absorption is obtained. In this context, the vibration reduction problem is formulated as a mathematical optimization problem subject to appropriate constraints. Subsequently, the methodology used to achieve this objective will be detailed, for later experimental validation.

4.1. Objective Function and Optimization Problem. Previously, it was shown that the steady state amplitude of the primary system with autoparametric cantilever beam absorber
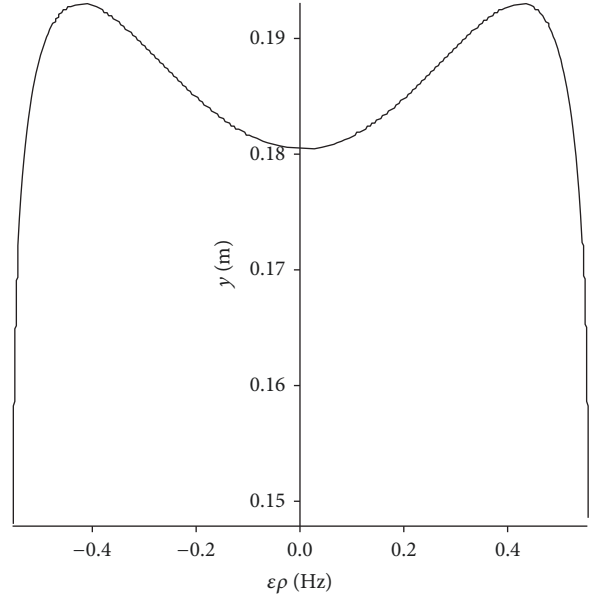
is given by (15). It is important to note that if we have an exact tuning condition ($\varepsilon \rho_1 = 0$ and $\omega_1 = 2\omega_2$), (15) becomes

$$a = \frac{1}{\varepsilon g} \left(\varepsilon \zeta_2 \right), \tag{18}$$

where $\varepsilon g = 6/5l$ and $\varepsilon \zeta_2 = c_2/2m\omega_2$. Substituting these expressions into (18) gives the following result:

$$a = \frac{5c_2 l}{12 m \omega_2}, \tag{19}$$

but $\omega_2 = \sqrt{k_{\text{beam}}/m}$; therefore (19) becomes

$$a = \frac{5c_2 l \sqrt{l^3 m}}{12 \sqrt{3EIm}}. \tag{20}$$

After performing the relevant algebraic manipulations, the steady state amplitude of the primary system with nonlinear absorber can be expressed as

$$a = \alpha l^{5/2} m^{-1/2}, \tag{21}$$

where $\alpha = 5c_2/12\sqrt{3EI}$.

On the other hand, it is well known that for the presence of autoparametric interaction between primary system and nonlinear absorber it is necessary to satisfy the following frequency relation:

$$\omega_2 = \frac{\omega_1}{2} \tag{22}$$

which implies that

$$\sqrt{\frac{3EI}{l^3 m}} = \frac{\omega_1}{2} \tag{23}$$

and thus

$$m = \frac{12EI}{\omega_1^2 l^3} = \beta l^{-3}, \qquad (24)$$

where $\beta = 12EI/\omega_1^2$. Now, substituting (24) in (21), the proposed objective function is gotten and it is represented by

$$a(l) = \gamma l^4, \qquad (25)$$

where $\gamma = \alpha/\beta^{1/2} = 5c_2\omega_1/72EI$.

In this way, the optimization problem to solve can be formulated as one that minimizes the following function:

$$\min_{l_{min} \le l_{beam} \le l_{max}} a(l) \qquad (26)$$

subject to the following physical constraint:

$$0.45 \text{ m} \le l \le 0.8 \text{ m}. \qquad (27)$$

4.2. Optimization Problem Solution. Now, the formulation of the nonlinear vibration absorber optimization problem consists of several ingredients: the objective function (26), constraints (27), and design variables (m, l). In order to solve the optimization problem given by (26), the Karush–Kuhn–Tucker (KKT) conditions are used. These conditions can be regarded as optimality conditions for both variational inequalities and constrained optimization problems [23]. This way, the Lagrange function is defined

$$L(l, \lambda) = a(l) + \sum_{i=1}^{m} \lambda_i g_i(l), \qquad (28)$$

where $a(l)$ is the proposed objective function, λ_i are Lagrange operators, and $g_i(l)$ are inequality constraints. Therefore, the Lagrange function is represented by

$$L(l, \lambda) = \gamma l^4 + \lambda_1(l - 0.45) + \lambda_2(-l + 0.8). \qquad (29)$$

4.2.1. First Condition. The KKT first condition states that

$$\frac{\delta a(l^*)}{\delta l_j} + \sum_{i=1}^{m} \lambda_i^* \frac{\delta g_i(l^*)}{\delta l_i} = 0 \quad \text{for } j = 1, \ldots, m, \qquad (30)$$

where l^* is optimal length of the nonlinear absorber (i.e., the solution to (27)). By developing (30), it results that

$$4\gamma l^3 + \lambda_1 - \lambda_2 = 0. \qquad (31)$$

4.2.2. Second Condition. The KKT second condition states that

$$g_i(l^*) \ge 0 \quad \text{for } i = 1, \ldots, m; \qquad (32)$$

it means

$$l^* - 0.45 \ge 0,$$
$$-l^* + 0.8 \ge 0. \qquad (33)$$

4.2.3. Third Condition. This condition yields that all values of Lagrange operators which are gotten when (27) is solved must be less than or equal to cero, so we have

$$\lambda_1 \le 0,$$
$$\lambda_2 \le 0. \qquad (34)$$

4.2.4. Fourth Condition. The KKT fourth condition states that

$$\lambda_i^* g_i(l^*) = 0 \quad \text{for } i = 1, \ldots, m, \qquad (35)$$

which yields

$$\lambda_1(l - 0.45) = 0,$$
$$\lambda_2(-l + 0.8) = 0. \qquad (36)$$

With the application of KKT condition, a nonlinear equations system is obtained, which is given by

$$4\gamma l^3 + \lambda_1 - \lambda_2 = 0,$$
$$\lambda_1(l - 0.45) = 0, \qquad (37)$$
$$\lambda_2(-l + 0.8) = 0.$$

It is necessary to solve (37) in order to get the solution of (26) which guarantees the optimum vibration absorption between primary system and nonlinear absorber.

Because of KKT third condition (34), the four possible solutions which can be obtained when trying to solve (37) are

$$\lambda_1 = \lambda_2 = 0, \qquad (38)$$

$$\lambda_1 < 0,$$
$$\lambda_2 < 0, \qquad (39)$$

$$\lambda_1 = 0,$$
$$\lambda_2 < 0, \qquad (40)$$

$$\lambda_1 < 0,$$
$$\lambda_2 = 0. \qquad (41)$$

The possible solution proposed by (38) cannot be gotten since it implies $4\gamma l^3 = 0$, but this term will be always positive. Equation (39) leads to a contradiction because the solution of (37) would be $l = 0.45$ m and $l = 0.80$ m. The third possible option represented by (40) cannot be fulfilled either since it would result in a value of $\lambda_2 = 4\gamma l^3$, but this term must be negative under this condition.

Finally, the solution of (37) is gotten when (41) is considered. This condition means that $\lambda_1 < 0$ and $\lambda_2 = 0$; therefore system (37) becomes

$$4\gamma l^3 + \lambda_1 - \lambda_2 = 0,$$
$$l - 0.45 = 0. \qquad (42)$$

TABLE 2: Meaning of the parameters used in the optimization algorithm.

Symbol	Description
ω_1	Natural frequency of the primary system
ω_2	Natural frequency of the nonlinear absorber
m	Tip mass of the cantilever beam
c_2	Viscous damping coefficient of the secondary system
ζ_2	Damping factor of the secondary system
l	Length of the cantilever beam
k_{beam}	Stiffness of the cantilever beam
E	Modulus of Young (aluminum)
I	Area moment of inertia
λ_i	Lagrange operators
g_i	Inequality constraints
l^*	Optimal length of the nonlinear absorber

TABLE 3: Experimental system parameters.

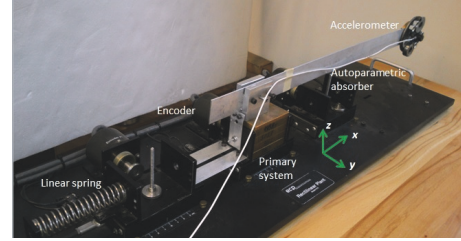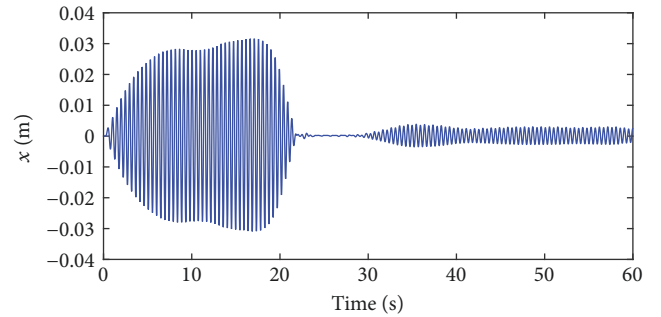|	
$M = 3.905\,\text{kg}$	$k = 726\,\text{N/m}$
$c_1 = 4.1872\,\text{N/(m/s)}$	$I_{\text{beam}} = 8.46825 \times 10^{-12}\,\text{m}^4$
$F_0 = 1.5\,\text{N}$	$E = 69\,\text{GPa}$

FIGURE 6: Experimental platform under passive control scheme.

FIGURE 7: Experimental response for the primary system obtained with the parameters of the first experiment.

It is clear that $l = 0.45\,\text{m}$ and $\lambda_1 = -4\gamma l^3$ (complying with the condition imposed by (41)); besides it is known that (24) provides the value of mass m associated with the secondary system in terms of its length, so, this way, the parameters that guarantee the highest percentage of vibration absorption in the primary system under resonant condition have been obtained.

In summary, the Karush–Kuhn–Tucker (KKT) conditions play an important role in optimization. In a few special cases it is possible to solve the KKT conditions (and, therefore, the optimization problem) analytically (as the authors state in this section). More generally, many algorithms for convex optimization are conceived as, or can be interpreted as, methods for solving the Karush–Kuhn–Tucker (KKT) conditions.

4.3. List of Symbols. Due to the number of variables implemented in the optimization strategy developed, Table 2 provides the list of symbols and notation used.

4.4. Experimental Results with Passive Nonlinear Absorber. In order to validate the optimum design of the autoparametric cantilever beam absorber proposed in previous section, a rectilinear plant (model 210a) provided by *Educational Control Products©* is used. The configuration of the primary system consists of one mass carriage (M), connected to the base by an helical spring with constant pitch (see Figure 6).

The mass carriage suspension has an antifriction ball bearing system and, therefore, the linear dashpot (c_1) is included only to describe the presence of a small (linear) viscous damping. The external force is obtained from a brushless-type servo motor connected to a pinion-rack mechanism. In the mass carriage there exists high resolution optical encoders to measure their actual positions via cable-pulley systems. The parameters of the primary system used during the development of the experiments as well as certain physical characteristics associated with the autoparametric cantilever beam absorber are given in Table 3.

A serie of experiments were performed to support the theoretical results shown before. The first pair of experiments were carried out with arbitrary parameters in the secondary system, where the only restriction was that (5) and (6) were satisfied in order to guarantee autoparametric interaction between primary system and nonlinear absorber, hence mechanical vibration absorption. The dynamic behavior of both experiments is shown in Figures 7 and 8, respectively. It can be emphasized that although the passive control scheme dissipates much of the external energy supplied to the primary system through the autoparametric cantilever beam absorber, its optimal performance is not yet achieved.

It is during the implementation of the third experiment when the steady state amplitude of the primary system is minimized while the optimal parameters of the autoparametric absorber were used to perform it. Figure 9 describes the dynamic behavior of the main mass when the autoparametric cantilever beam absorber has the optimal length and mass. A comparison of the performance obtained in each experiment implemented is given in Table 4. Finally, a zoomed visualisation during the last seconds of the time history response of the primary system considering the experiments carried out is shown in Figure 10, where it is clear that the objective set out in (26) has been achieved.

TABLE 4: Comparative table of experimental results.

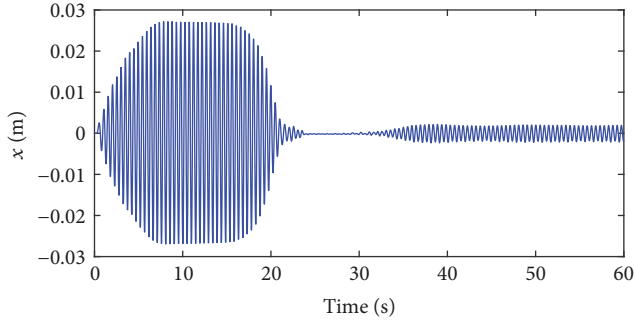| Experiment	Main parameters	Nonlinear absorber	Steady state amplitude	Vibration absorption
1	$m = 0.23\,\text{kg}$	$L = 0.542\,\text{m}$	3.07 mm	88.9%
2	$m = 0.31\,\text{kg}$	$L = 0.504\,\text{m}$	1.81 mm	93.5%
3	$m = 0.47\,\text{kg}$	$L = 0.450\,\text{m}$	1.56 mm	94.4%

FIGURE 8: Experimental response for the primary system obtained with the parameters of the second experiment.
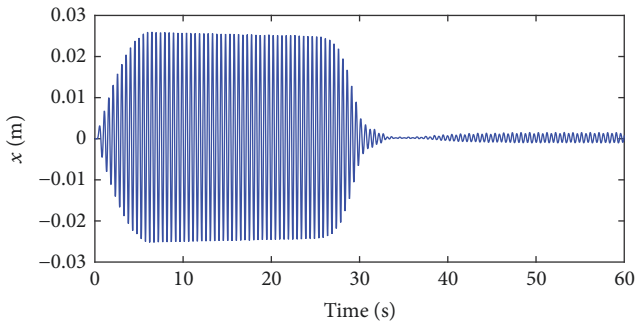

FIGURE 9: Experimental response for the primary system obtained with the optimal parameters.

— Optimal parameters
— Second experiment
— First experiment

FIGURE 10: Steady state response comparison of the primary system.

Remark 1. The main contribution of an autoparametric vibration absorber is that it only works exactly or close to the so-called principal parametric resonance frequency (design frequency) associated with the primary system. Hence, an autoparametric absorber does not introduce more resonant peaks on the overall system response, in contrast to classical Dynamical Vibration Absorber or Tuned Mass Dampers [24].

5. System with Active Nonlinear Absorber

In case the excitation frequency Ω in the perturbation force $F(t)$ is unknown or time varying, the nonlinear absorber may not be useful for vibration absorption in the primary system. However, when the excitation frequencies change such that $\Omega \neq \omega_1$, one is still able to satisfy the internal tuning condition $\omega_1 = 2\omega_2$ in order to get some attenuation of the primary system response.
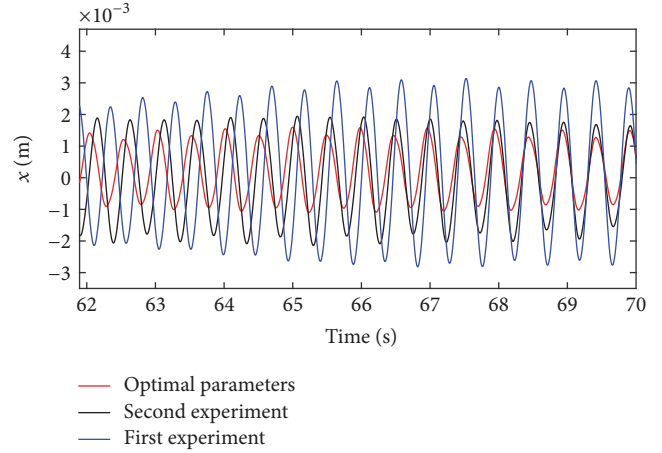
The equations of motion for the two-degree-of-freedom system consisting of the primary system and the active autoparametric cantilever beam absorber are expressed as follows:

$$(M + m)\,\ddot{x} + c_1\dot{x} + kx - \frac{6m}{5l}\left(y\ddot{y} + \dot{y}^2\right) = F(t), \quad (43)$$

$$m\ddot{y} + c_2\dot{y} + \left(\frac{3EI}{l^3} - \frac{6m}{5l}\ddot{x}\right)y + \frac{36m}{25l^2}y\left(y\ddot{y} + \dot{y}^2\right)$$
$$= u(t). \quad (44)$$

The equivalent control force acting on the Euler–Bernoulli cantilever beam (44) is obtained as

$$u(t) = BM_p = Bg_aV, \quad (45)$$

where V is the voltage applied between the electrodes of the PZT layer, B is the so-called influence vector, and $g_a = -e_{31}bz_m$ is the actuator gain, which can be calculated from the PZT parameters as material properties and patch size. Here e_{31} is a PZT constant ($e_{31} = -7.5\,\text{Coulomb/m}^2$) and b is the constant electrode width [25]. The active vibration control can be achieved by using an appropriate control law on the PZT patch actuator, thus modifying the equivalent beam stiffness.

It is important to note that, when the frequency response function (15) is parameterized in terms of the equivalent stiffness k_c, provided by the smart actuator, it results in
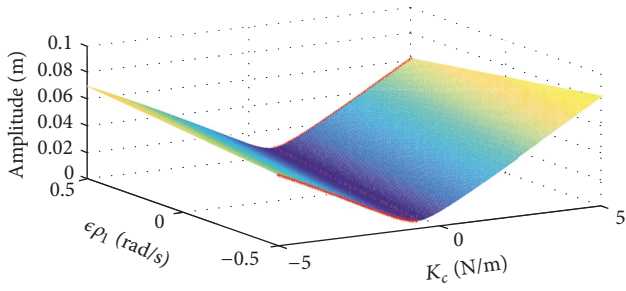
FIGURE 11: Parameterized FRF of the primary system in terms of the PZT actuator stiffness $k_c \in [-5, 5]$ N/m.

$$a = \frac{4}{(\varepsilon g)\,\omega_1^2} \sqrt[2]{\frac{1}{m}\left(\frac{3EI}{L^3} + k_c\right)\left[0.25\,(\varepsilon\rho_1 + \omega_1)^2 - \sqrt[2]{\frac{1}{m}\left(\frac{3EI}{L^3} + k_c\right)}(\varepsilon\rho_1 + \omega_1) + \frac{1}{m}\left(\frac{3EI}{L^3} + k_c\right) + \frac{0.25 c_2^2}{m^2}\right]}. \quad (46)$$

the approximate frequency response described in Figure 11 which is obtained via (46). Here, the nonlinear steady state amplitude (15) is shown in terms of $\varepsilon\rho_1$ and a reasonable range of the PZT actuator stiffness k_c, obtained by a simple proportional control law, in such a way that the internal resonance condition (6) can be satisfied to get the minimal attenuation gain. This information will be used to achieve an optimal attenuation operation for the autoparametric cantilever beam absorber. In fact, there exists some region with minimal amplitudes, which can be computed to guarantee the optimal attenuation tuning for the passive/active vibration absorber.

The passive/active control objective for the autoparametric cantilever beam absorber with PZT actuator is stated as follows:

(1) Given an excitation frequency Ω, compute the optimal attenuation stiffness constant $k_c^*(\Omega)$ for the PZT patch actuator, which minimizes the steady state amplitude of the primary system a for the passive vibration absorber; that is,

$$\min_{k_{cmin} \le k_c \le k_{cmax}} |a(\Omega, k_c)|, \quad (47)$$

where $a(\Omega, k_c)$ denotes the steady state amplitude in (15) parameterized in terms of Ω and k_c, for the closed interval $[k_{cmin}, k_{cmax}]$ associated with the physical limitations of the PZT actuator. This solution is computed numerically. For practical purposes the optimal stiffness $k_c^*(\Omega)$ can be computed and parameterized in terms of the excitation frequency Ω using curve fitting techniques on the data shown in Figure 11.

(2) With the knowledge of the optimal attenuation stiffness $k_c^*(\Omega)$ synthesizes a proportional state feedback and feedforward control law to get the automatic tuning of the autoparametric cantilever beam absorber:

$$u(t) = -k_c^*(\Omega)\, y(t). \quad (48)$$

Once the proportional controller (48) is activated, the steady state response of the active control system converges to the passive performance and, therefore, the control efforts are small compared to a fully active vibration control approach.

Note that, the above control law is easy to implement and combine with an optimal attenuation criterion. In fact, the main idea is that the equivalent stiffness on the cantilever beam absorber can be controlled in order to get the best tuning condition for resonant vibrations.

5.1. Experimental Results with Active Absorber.

In order to illustrate the dynamic performance of the passive/active cantilever beam vibration absorber, when the excitation frequency is changing between two different constant values, we use the system parameters in Table 3. The main actuator on the system is a piezoelectric patch made by *Physik Instrumente*© model P-876.A15. This is connected to a voltage amplifier (model E-413) type *DuraAct*©, which can drive the patch. This patch can be seen properly cemented on the basis of the cantilever beam (see Figure 12). The reason for such a place is that on the basis of the cantilever beam the bending stresses achieve the highest values. For control purposes a displacement signal has to be gathered and this is accomplished with the use of a strain gage at the bottom of the beam, whose instrumentation is made for a data acquisition system *National Instruments*© model NI cDAQ-9172-9236; then this signal is sent to the high-speed DSP board using the NI 9263 module.

The initial conditions are set to $x(0) = 0$ m, $y(0) = 0.005$ m, $\dot{x}(0) = 0$ m/s, and $\dot{y}(0) = 0$ m/s. The harmonic force $F(t) = F_0 \cos(\Omega t)$ is started with $F_0 = 1.5$ N and excitation frequency $\Omega = \omega_1 = 2.17$ Hz (i.e., $\varepsilon\rho_1 = 0$ rad/s).

Figure 13 describes the dynamic behavior of the overall closed-loop system (43)-(44) with the proportional control law (48), which includes the primary system, the passive/active cantilever beam absorber with PZT actuator. Before $t = 45$ s, the overall system is working in its passive form (i.e., $u \equiv 0$), with excitation frequency $\Omega_1 = \omega_1 = 2.17$ Hz and $\omega_2 = 1.085$ Hz. At $t = 45$ s, the excitation frequency is increased to $\Omega = 2.193$ Hz ($\varepsilon\rho_1 = +0.15$ rad/s). Here, one can observe that after a transient period of about 15 s, the primary system achieves the steady state condition with small amplitudes.

Another experimental result is shown in Figure 14; here, at $t = 45$ s, the excitation frequency changes from $\Omega_1 = 2.17$ Hz to $\Omega_1 = 2.138$ Hz ($\varepsilon\rho_1 = -0.2$ rad/s). Note how the primary system has a robust steady state amplitude after a brief transient period.
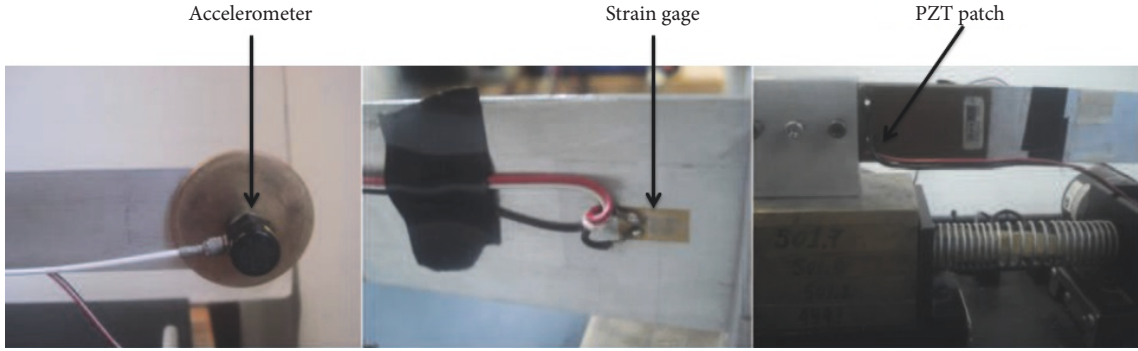
FIGURE 12: Details of the experimental platform under active control scheme: accelerometer, strain gage, and PZT patch.
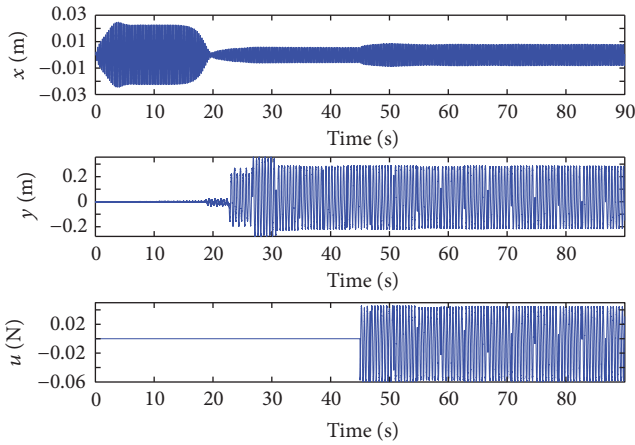

FIGURE 13: Dynamic response of the primary system, with autoparametric interaction, using the passive/active beam absorber and PZT actuator switching the stiffness feedback exactly at the frequency change ($\varepsilon\rho_1 = +0.15$ rad/s).
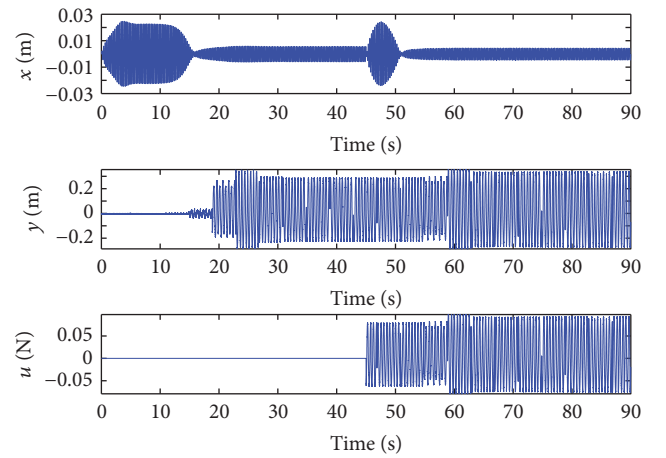

FIGURE 14: Dynamic response of the primary system, with autoparametric interaction, using the passive/active beam absorber and PZT actuator switching the stiffness feedback exactly at the frequency change ($\varepsilon\rho_1 = -0.2$ rad/s).

Basically, from Figures 13 and 14 it can be established that the active control law on the smart actuator makes it possible to automatically tune the nonlinear absorber in a robust sense, employing small control efforts and energy. Besides, the autoparametric nonlinear absorber is simultaneously passive and active, working as a passive absorber when the excitation frequency is exactly the computed tuning frequency and as an active absorber in any other condition. Finally, it is also important to note that in case of large variations on the excitation frequency Ω, the external resonance condition (5) is no longer valid and, hence, the mass-spring-damper system response is affected according to the first-mode operation described by the typical linear oscillator frequency response, thus making the nonlinear vibration absorber useless [26, 27].

6. Conclusions

In this paper, we have described the optimum design of a passive autoparametric vibration absorber applied to a linear mechanical system under resonant condition. The experimental comparison shows that the nonlinear absorber with the optimum parameters has the best performance to dissipate the external energy supplied to the primary system, justifying, in this way, the previous study in the nonlinear dynamics of the overall system via a perturbation method. On the other hand, The design of the active vibration control system is based on the previous design of the passive vibration absorber and the addition of a smart actuator to modify the equivalent beam stiffness in order to get an optimal attenuation steady state operation in case of varying excitation frequencies close to the principal parametric resonance. The active vibration scheme employs a simple proportional controller, which uses the measurements of the excitation frequency and the beam deflection. The overall dynamic performance proves the good robustness properties of the proposed control scheme for the attenuation in a nonlinear system with variable excitation frequencies close to the principal parametric resonant frequency. Further work is being performed to improve the transient response of the primary system, because this is a disadvantage of the autoparametric absorbers compared to the conventional Tuned Mass Damper (TMD) and/or Active Mass Damper (AMD).

Disclosure

The authors declare the partial presentation of this work in SPIE Smart Structures and Materials & Nondestructive Evaluation and Health Monitoring, 2013, San Diego, California, USA.

Conflicts of Interest

The authors declare that there are no conflicts of interest regarding the publication of this paper.

References

[1] D. J. Inman, *Vibration with Control*, Wiley, London, UK, 2006.

[2] J. P. Den Hartog, *Mechanical Vibration*, McGraw-Hill, New York, NY, USA, 1956.

[3] B. G. Korenev and L. M. Reznikov, *Dynamic Vibration Absorber: Theory and Technical Applications*, Wiley, London, UK, 1993.

[4] L. Zuo and S. A. Nayfeh, "Minimax optimization of multi-degree-of-freedom tuned-mass dampers," *Journal of Sound and Vibration*, vol. 272, no. 3–5, pp. 893–908, 2004.

[5] N. Hoang, Y. Fujino, and P. Warnitchai, "Optimal tuned mass damper for seismic applications and practical design formulas," *Engineering Structures*, vol. 30, no. 3, pp. 707–715, 2008.

[6] S. S. Oueini, A. H. Nayfeh, and J. R. Pratt, "A nonlinear vibration absorber for flexible structures," *Nonlinear Dynamics*, vol. 15, no. 3, pp. 259–282, 1998.

[7] S. S. Oueini and A. H. Nayfeh, "Analysis and application of a nonlinear vibration absorber," *Journal of Vibration and Control*, vol. 6, no. 7, pp. 999–1016, 2000.

[8] G. Kerschen, K. Worden, A. F. Vakakis, and J. Golinval, "Past, present and future of nonlinear system identification in structural dynamics," *Mechanical Systems and Signal Processing*, vol. 20, no. 3, pp. 505–592, 2006.

[9] R. A. Ibrahim, "Recent advances in nonlinear passive vibration isolators," *Journal of Sound and Vibration*, vol. 314, no. 3–5, pp. 371–452, 2008.

[10] A. Tondl, T. Ruijgrok, F. Verhulst, and R. Nabergoj, *Autoparametric Resonance in Mechanical Systems*, Cambridge University Press, Cambridge, MA, USA, 2000.

[11] R. S. Haxton and A. D. S. Barr, "The autoparametric vibration absorber," *Journal of Engineering for Industry*, vol. 94, no. 1, pp. 119–225, 1972.

[12] M. P. Cartmell and J. W. Roberts, "Simultaneous combination resonances in an autoparametrically resonant system," *Journal of Sound and Vibration*, vol. 123, no. 1, pp. 81–101, 1988.

[13] M. P. Cartmell and J. Lawson, "Performance enhancement of an autoparametric vibration absorber by means of computer control," *Journal of Sound and Vibration*, vol. 177, no. 2, pp. 173–195, 1994.

[14] O. Cuvalci and A. Ertas, "Pendulum as vibration absorber for flexible structures: experiments and theory," *Journal of Vibration and Acoustics*, vol. 118, no. 4, pp. 558–566, 1996.

[15] A. Vyas and A. K. Bajaj, "Dynamics of autoparametric vibration absorbers using multiple pendulums," *Journal of Sound and Vibration*, vol. 246, no. 1, pp. 115–135, 2001.

[16] B. Vazquez-Gonzalez and G. Silva-Navarro, "Evaluation of the autoparametric pendulum vibration absorber for a Duffing system," *Shock and Vibration*, vol. 15, no. 3-4, pp. 355–368, 2008.

[17] G. Silva-Navarro, H. F. Abundis-Fong, and B. Vazquez-Gonzalez, "Application of a passive/active autoparametric cantilever beam absorber with PZT actuator for Duffing systems," in *Proceedings of the Active and Passive Smart Structures and Integrated Systems 2013*, March 2013.

[18] G. Silva-Navarro and H. F. Abundis-Fong, "Passive/active autoparametric cantilever beam absorber with piezoelectric actuator for a two-story building-like structure," *Journal of Vibration and Acoustics*, vol. 137, no. 1, Article ID 011017, 2015.

[19] Z. Yan, H. E. Taha, and T. Tan, "Nonlinear characteristics of an autoparametric vibration system," *Journal of Sound and Vibration*, vol. 390, pp. 1–22, 2017.

[20] A. H. Nayfeh and D. T. Mook, *Nonlinear Oscillations*, John Wiley & Sons, New York, NY, USA, 1979.

[21] J. Kevorkian and J. D. Cole, *Multiple Scale and Singular Perturbation Methods*, Springer-Verlag, New York, NY, USA, 1996.

[22] R. S. Johnson, "Singular perturbation theory: Mathematical and analytical techniques with applications to engineering," *Singular Perturbation Theory: Mathematical and Analytical Techniques with Applications to Engineering*, pp. 1–292, 2005.

[23] J. Nocedal and S. J. Wright, *Numerical Optimization*, P. Glynn and S. M. Robinson, Eds., Springer-Verlag, New York, NY, USA, 1999.

[24] T. Dahlberg, "On optimal use of the mass of a dynamic vibration absorber," *Journal of Sound and Vibration*, vol. 132, no. 3, pp. 518–522, 1989.

[25] A. Preumont, *Mechatronics: Dynamics of Electromechanical and Piezoelectric Systems*, Springer, Dordrecht, Netherlands, 2006.

[26] B. F. Spencer and S. Nagarajaiah, "State of the art of structural control," *Journal of Structural Engineering-ASCE*, vol. 129, no. 7, pp. 845–856, 2003.

[27] M. Domaneschi, "Simulation of controlled hysteresis by the semi-active Bouc-Wen model," *Computers & Structures*, vol. 106-107, pp. 245–257, 2012.